Supporting Information

© Copyright Wiley-VCH Verlag GmbH & Co. KGaA, 69451 Weinheim, 2019

Commensurate $Nb_2Zr_5O_{15}$: Accessible Within the Field $Nb_2Zr_xO_{2x+5}$ After All

Dennis Wiedemann,* Steven Orthmann, Martin J. Mühlbauer, and Martin Lerch© 2019 The Authors. Published by Wiley-VCH Verlag GmbH & Co. KGaA.
This is an open access article under the terms of the Creative Commons Attribution Non-Commercial License, which permits use, distribution and reproduction in any medium, provided the original work is properly cited and is not used for commercial purposes.

Content

1 Detailed Experimental Procedures

1.1 Synthesis

Ternary oxides were synthesized *via* a modified PECHINI sol–gel route.[1] Citrate solutions were prepared by dissolving citric acid (Sigma-Aldrich, ≥99.5%; r = 12:1 based on metal) and either hafnium(IV) (Alfa Aesar, 99.9%), niobium(V) (Sigma-Aldrich, 99.999%), tantalum(V) (Sigma-Aldrich, 99.999%), or zirconium(IV) chloride (Sigma-Aldrich, 99.99%) in absolute ethanol (Acros Organics, 99.5%). Aliquots of both solutions according to the pursued cation ratio were combined and mixed with ethylene glycol (Alfa Aesar, 99%; $\psi \approx 2{:}1$). The resulting solution (*ca.* 100 mL) was polymerized at 200 °C in an alumina crucible in a chamber furnace. After calcination at 400 °C for 18 h, an—according to X-ray diffraction—amorphous powder was obtained. The temperature was then increased to 800 °C for another 18 h to obtain the product as a slightly off-white powder (typically 0.5–0.7 g).

For comparison to published protocols, we also tried to synthesize $Nb_2Zr_5O_{15}$ *via* a solid-state route. For this purpose, Nb_2O_5 (Alfa Aesar, 99.9985%; 301.4 mg, 1.134 mmol) and ZrO_2 (Alfa Aesar, 99.7%; 698 mg, 5.669 mmol) were mixed and placed in an alumina crucible. The latter was then heated to 1500 °C in a chamber furnace with a rate of 300 °C/h and kept at that temperature for 12 h. After cooling down to below 100 °C within 5 h, a mixture of an α-PbO_2-homeotypic niobium zirconium oxide, baddeleyite-type ZrO_2, and an unidentified minor phase was acquired as a white powder.

1.2 Analytical Methods

The oxygen content was determined using a "Leco EF-TC 300" N_2/O_2 analyzer (hot-gas extraction). Volumetric mass density was measured using a "Quantachrome Multipycnometer" gas expansion pycnometer fed with helium (sample volume: 4.5 cm^3).

1.3 Neutron Diffraction

Measurement was carried out at FRM II (Heinz Maier-Leibnitz Zentrum, Garching b. München) using the high-resolution powder diffractometer SPODI with Ge(551)-monochromated neutron radiation (λ = 1.54829 Å) in DEBYE–SCHERRER geometry.[2] The compacted powder sample was mounted in a vanadium cylinder and exposed for *ca.* 7 h. Profile data were recorded stepwise with an array of 80 position-sensitive ^{3}He tubes ($2\theta_{max}$ = 160°, effective height: 300 mm) and reduced using a variable-height algorithm as implemented in the in-house parser,[3] yielding a final range of $0.95° \leq 2\theta \leq 151.90°$ with $\Delta(2\theta) = 0.05°$.

All following calculations were carried out using JANA2006.[4] Neutron data were analytically corrected for absorption (cylindrical sample, μ_{calc} = 0.0007 mm^{-1}, $\mu_{calc}R$ = 0.006) and stripped of the steep onset below 10°. Peak profiles were fitted with a pseudo-VOIGT function using the

THOMPSON–COX–HASTINGS approach (GAUSSian parameters *U*, *V* [both fixed at values from the instrument resolution function], and *W*; LORENTZian parameters *X* and *Y*). Asymmetry due to axial divergence was corrected for using the FINGER–COX–JEPHCOAT method with fixed values from the instrument resolution function.[5] A zero-shift correction was refined. The background was modelled using 15 LEGENDRE polynomials between 25 manually defined points. Satellite reflections up to the second order were taken into account.

Initial LE-BAIL fits showed anisotropic reflection broadening (caused by variations of lattice and modulation parameters) that was in turn treated with a strain-type model.[6] For subsequent RIETVELD refinement against intensity data, the atomic model of $Hf_3Ta_2O_{11}$ based on neutron diffraction was imported.[7] The composition and the occupancy modulation of O3 were adjusted. A scale factor was introduced. Initially, profile parameters were kept fixed while atomic parameters were successively freed. A critical inspection of DE-WOLFF sections led to a reduction of the positional modulation parameters of O2 to four (first order for all principal directions, second order for *z*). Data allowed refining anisotropic displacement for the cation without modulation and isotropic displacement for the oxide ions O1 and O2. For O3, the displacement had to be fixed at U_{iso} = 0.0067 Å^2 (average of the anions). Finally, profile parameters were freed and all insignificant broadening parameters ($S'_{HKLM} < 3\sigma[S'_{HKLM}]$) were successively set to zero and excluded from refinement. The final model was thus refined with one scale, 15 background, one shift, three profile, ten broadening (see Table S1), three cell, seven positional, five displacement, and ten positional modulation parameters. Structure graphics were produced using DIAMOND 4.5.[8]

Table S1. Refined Parameters for Anisotropic Reflection Broadening.

Parameter	Value
S'_{4000}	2.46(14)
S'_{2200}	–0.36(2)
S'_{0220}	–0.54(5)
S'_{0040}	–0.92(8)
S'_{0211}	–1.55(16)
S'_{0031}	–3.9(4)
S'_{2002}	23.7(9)
S'_{0202}	7.1(4)
S'_{0022}	17.6(9)
ζ	0.651(19)

CCDC 1893626–1893627 contain the supplementary crystallographic data for this paper. These data can be obtained free of charge from FIZ Karlsruhe *via* https://www.ccdc.cam.ac.uk/structures.

1.4 X-Ray Diffraction

Measurements were carried out at ambient temperature on a "PANalytical X'Pert PRO MPD" diffractometer in BRAGG–BRENTANO (θ–θ) geometry equipped with a "PIXcel" detector using nickel-filtered Cu-K_α radiation (λ_1 = 1.54056 Å, λ_2 = 1.54439 Å, I_2/I_1 = 0.5).

All calculations were carried out using JANA2006.[4] In an initial LE-BAIL fit, peak profiles were modelled with a pseudo-VOIGT function using the THOMPSON–COX–HASTINGS approach (GAUSSian parameters U, V, and W; LORENTZian parameter X). Asymmetry was corrected for using the BÉRAR–BALDINOZZI method with two parameters.[9] Displacement and transparency corrections were applied. The background was modelled using Legendre polynomials between manually defined points. Satellite reflections up to the second order were used.

In subsequent RIETVELD refinement, analytic expressions of ionic form factors were employed.[10] As a starting point, the final model from neutron diffraction was imported. Persistent instabilities, caused by shallow minima and very weak satellite reflections, made us choose the LEVENBERG–MARQUART algorithm (fudge factor: 0.001) and a damping factor of 0.75 throughout. As only one satellite reflection was even visually discernible, all modulation parameters had to be fixed (the refinement of $|\boldsymbol{q}|$ led to divergence). Data allowed refining anisotropic displacement for the cation and isotropic displacement for O1 and O2. The isotropic displacement parameter of O3 was fixed at U_{iso}(O3) = 0.025 Å^2 ≈ U_{iso}(O2). Due to the long measurement, a weak reflection of the silicon sample holder occurred at $2\theta \approx 33.0°$. This was remedied by taking a by-phase of the high-pressure silicon type into account (LE-BAIL fit; fixed profile parameters during RIETVELD refinement of main phase).

Results of RIETVELD refinements and diffractograms for comparison were plotted using ORIGINPRO 2018[11] and HIGHSCORE PLUS 4.8,[12] respectively.

2 Additional Crystal-Structural Information (Neutron Data)

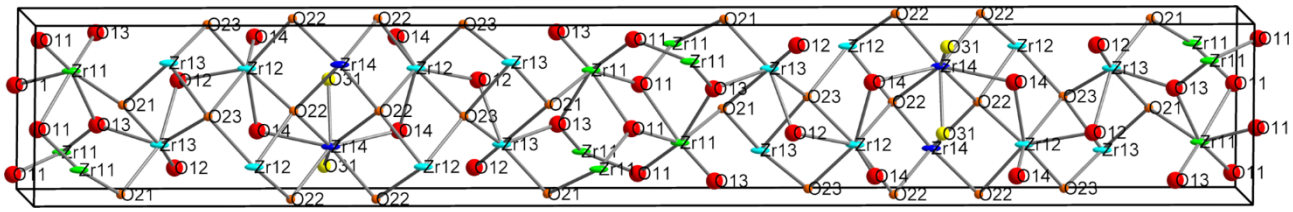

Figure S1. Crystal structure according to neutron diffraction. View approximately along [100], atoms as displacement ellipsoids/spheres of 90% probability, unit cell (supercell model) in black, identical niobium and zirconium positions.

3 DE-WOLFF Sections (Neutron Data)

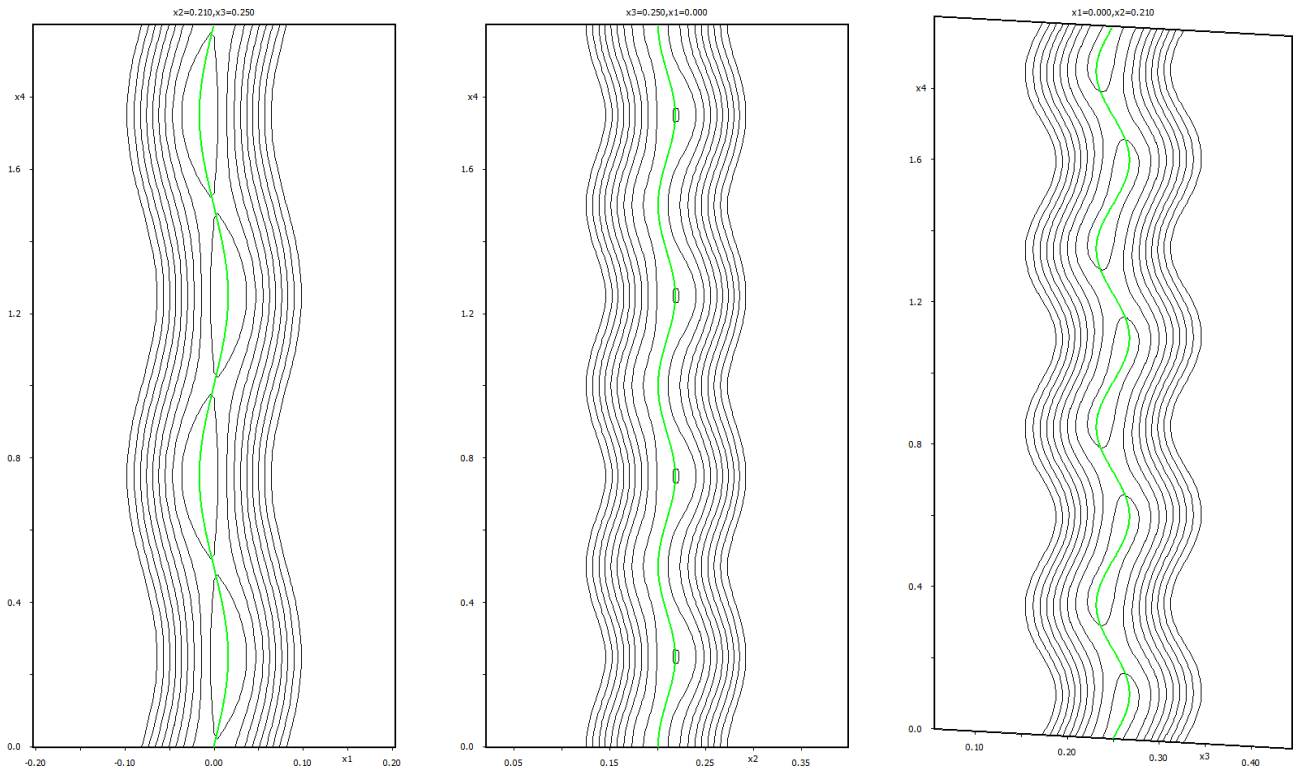

Figure S2. DE-WOLFF sections for Hf1/Ta1 (green line) summed over a secondary-coordinate range of 1 Å. Plot of uniform contours with $\Delta\rho$ = 2 fm Å^{-3}; $x_1 = x$, $x_2 = y$, $x_3 = z$.

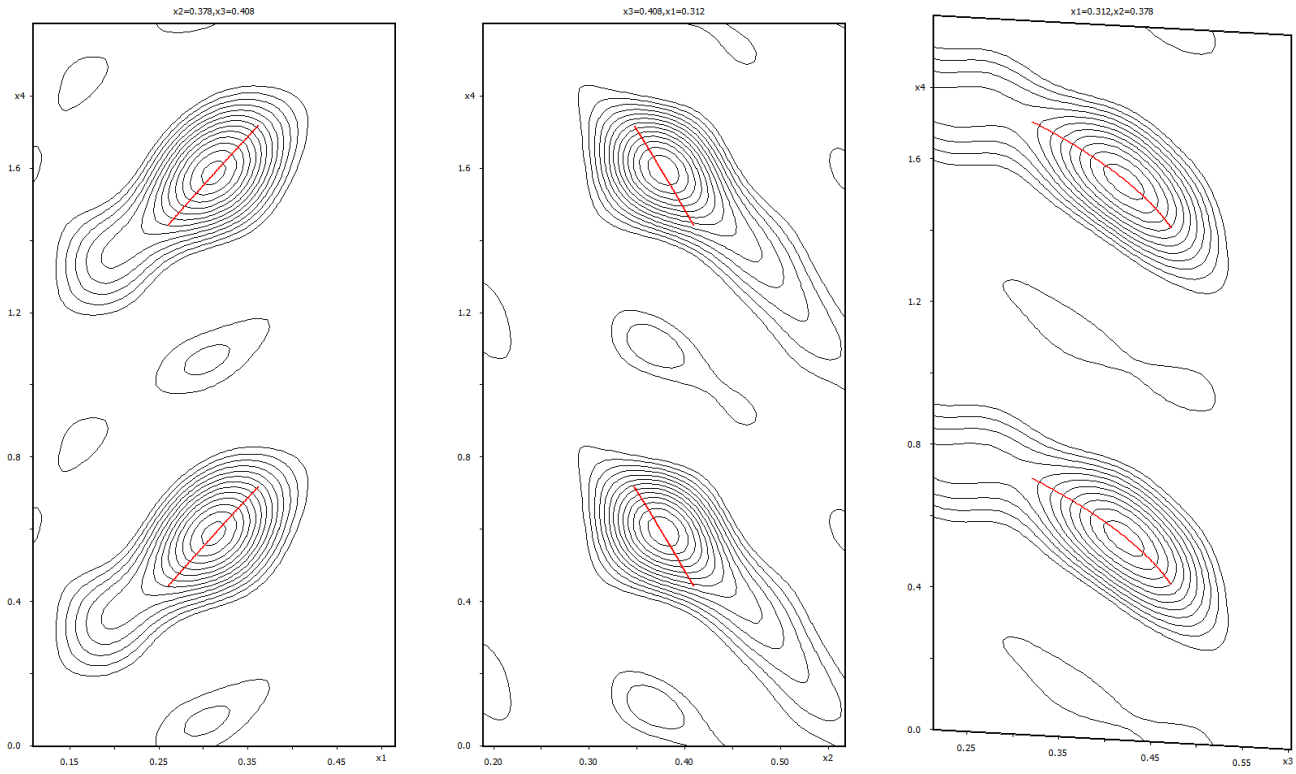

Figure S3. DE-WOLFF sections for O1 (red line) summed over a secondary-coordinate range of 1 Å. Plot of uniform contours with $\Delta\rho$ = 1 fm Å^{-3}; $x_1 = x$, $x_2 = y$, $x_3 = z$.

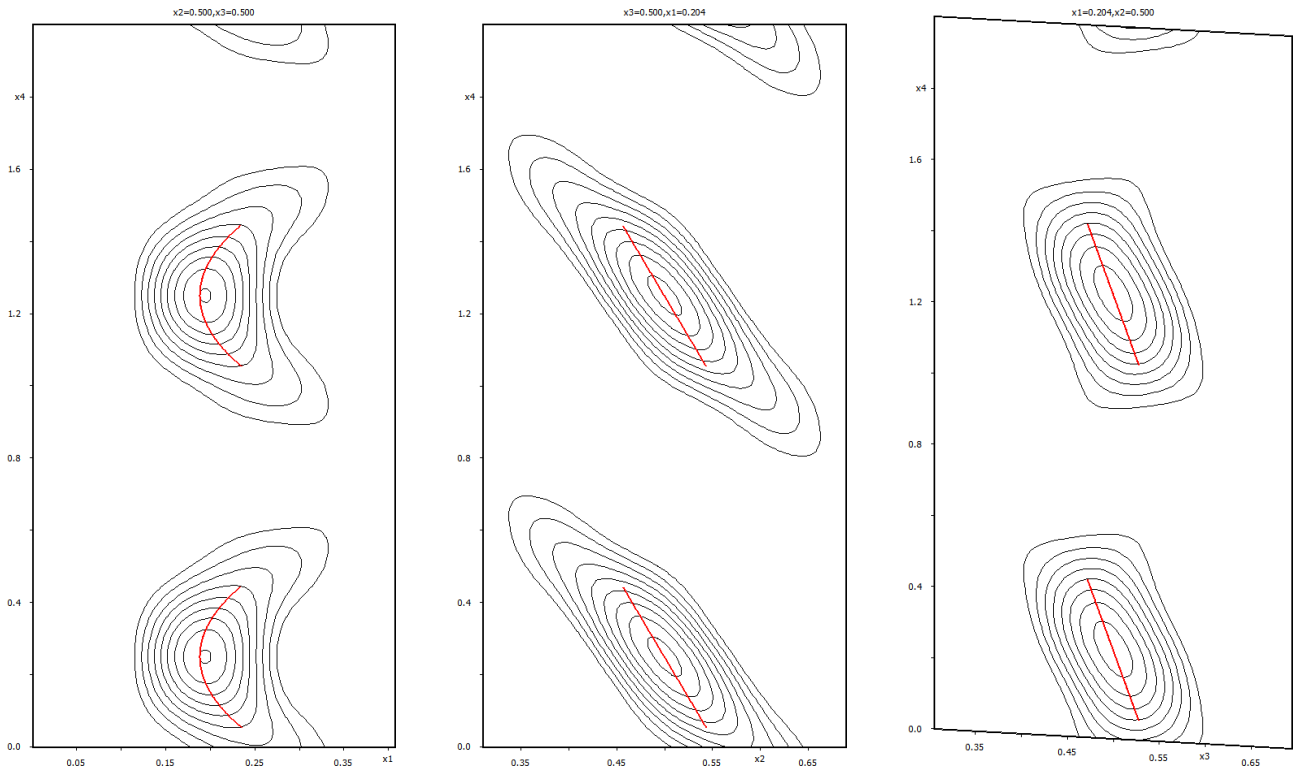

Figure S4. DE-WOLFF sections for O2 (red line) summed over a secondary-coordinate range of 1 Å. Plot of uniform contours with $\Delta\rho$ = 2 fm Å^{-3}; $x_1 = x$, $x_2 = y$, $x_3 = z$.

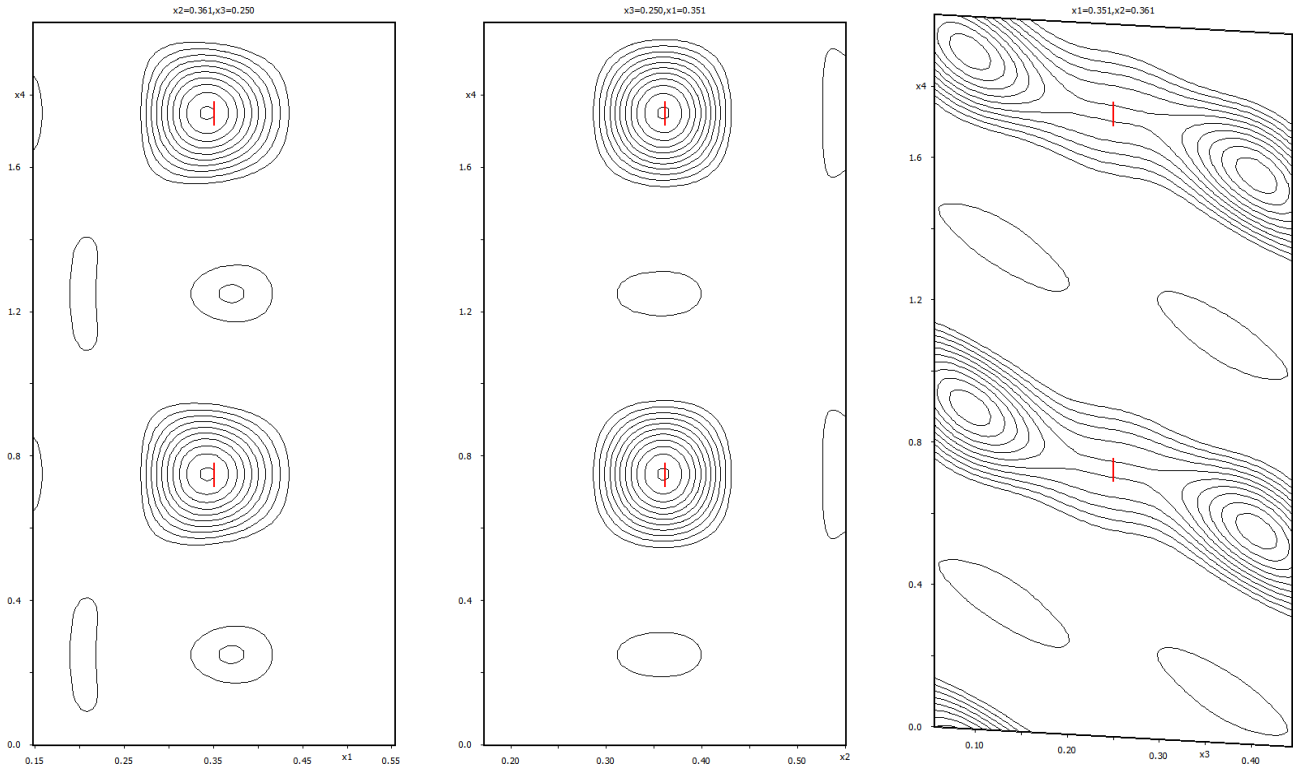

Figure S5. DE-WOLFF sections for O3 (red line) summed over a secondary-coordinate range of 1 Å. Plot of uniform contours with $\Delta\rho$ = 1 fm Å^{-3}; $x_1 = x$, $x_2 = y$, $x_3 = z$.

4 X-Ray Diffractograms

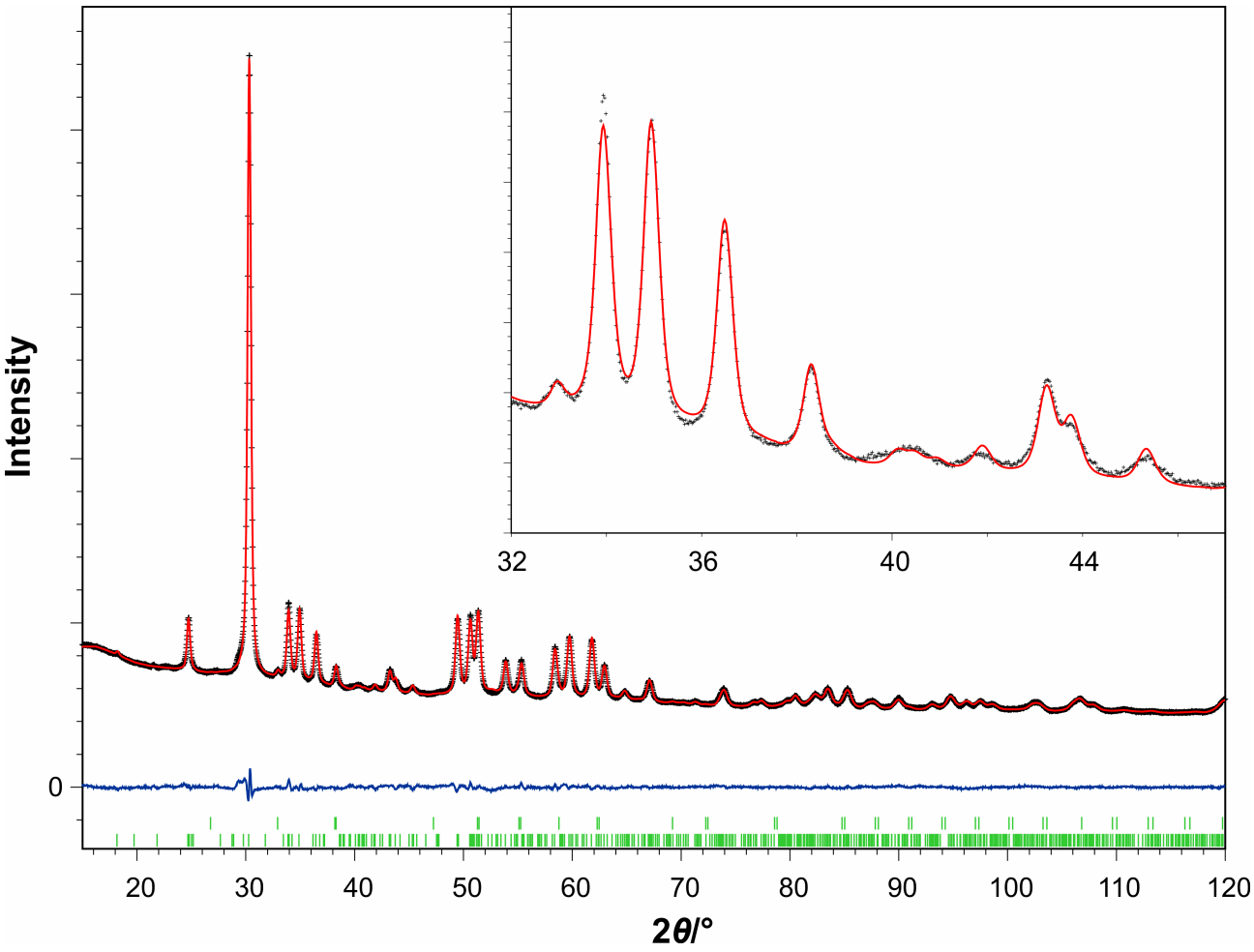

Figure S6. Diffractogram of $Nb_2Zr_5O_{15}$ sample with refinement results (modulation parameters unrefined; R_p = 0.0082, wR_p = 0.0110, R_{exp} = 0.0028, S = 3.85, R_F = 0.0311, wR_F = 0.0534, R_B = 0.0417). Red: calculated, black: observed, blue: difference density; green: BRAGG positions for $Nb_2Zr_5O_{15}$ (bottom) and Si sample holder (top). The inset shows a detail of a diagnostic region, in which the satellite reflections are dominant.

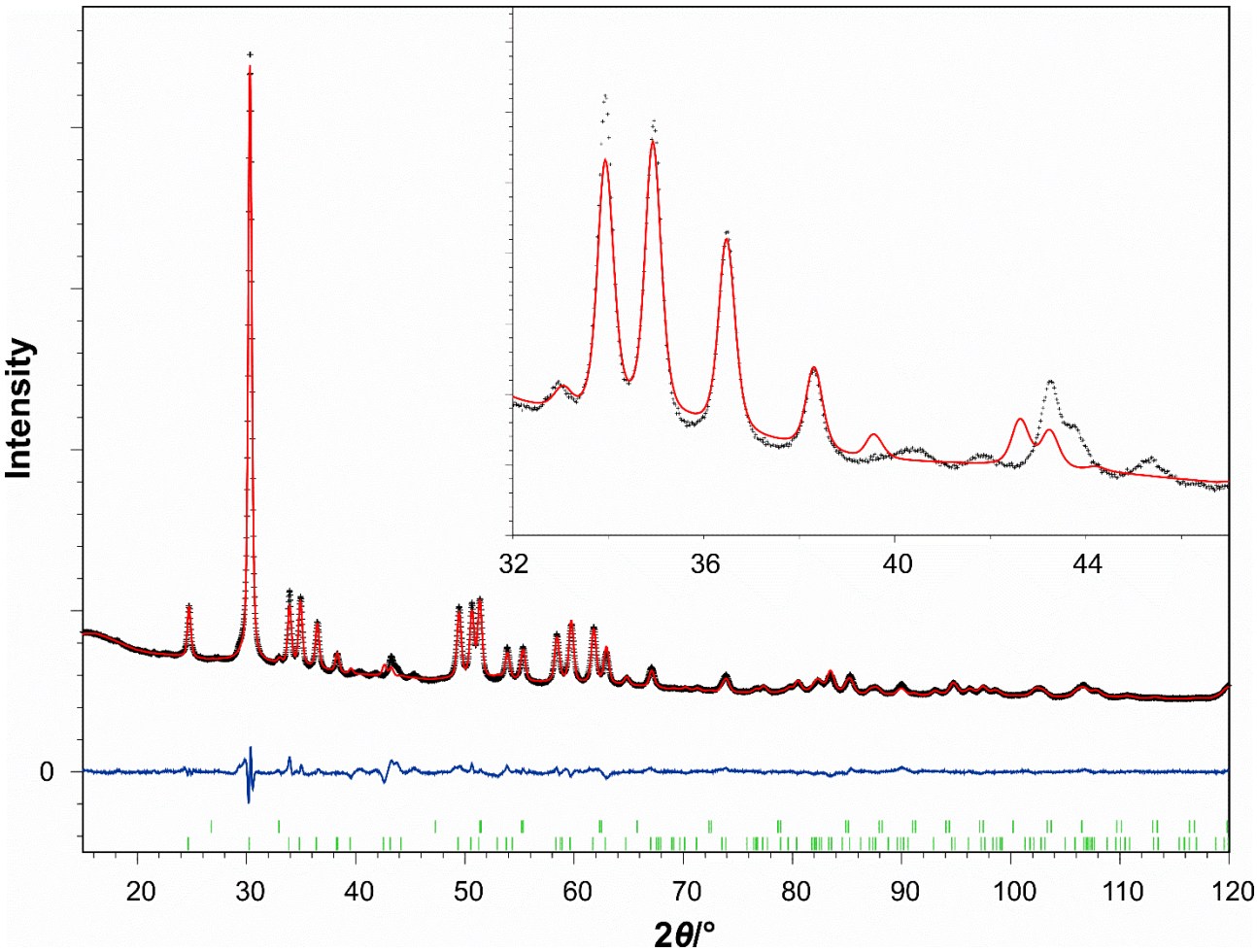

Figure S7. Refinement results of an α-PbO_2-type model of "$Nb_2Zr_5O_{14}$" (R_p = 0.0192, wR_p = 0.0197, R_{exp} = 0.0028, S = 6.91, R_F = 0.0593, wR_F = 0.1054, R_B = 0.0930). Red: calculated, black: observed, blue: difference density; green: BRAGG positions for "$Nb_2Zr_5O_{14}$" (bottom) and Si sample holder (top). The fit is significantly worse compared to the correct $Nb_2Zr_5O_{15}$ model (*cf.* Fig. S5). The inset shows a detail of a diagnostic region with an obvious misfit due to the disregard of modulation.

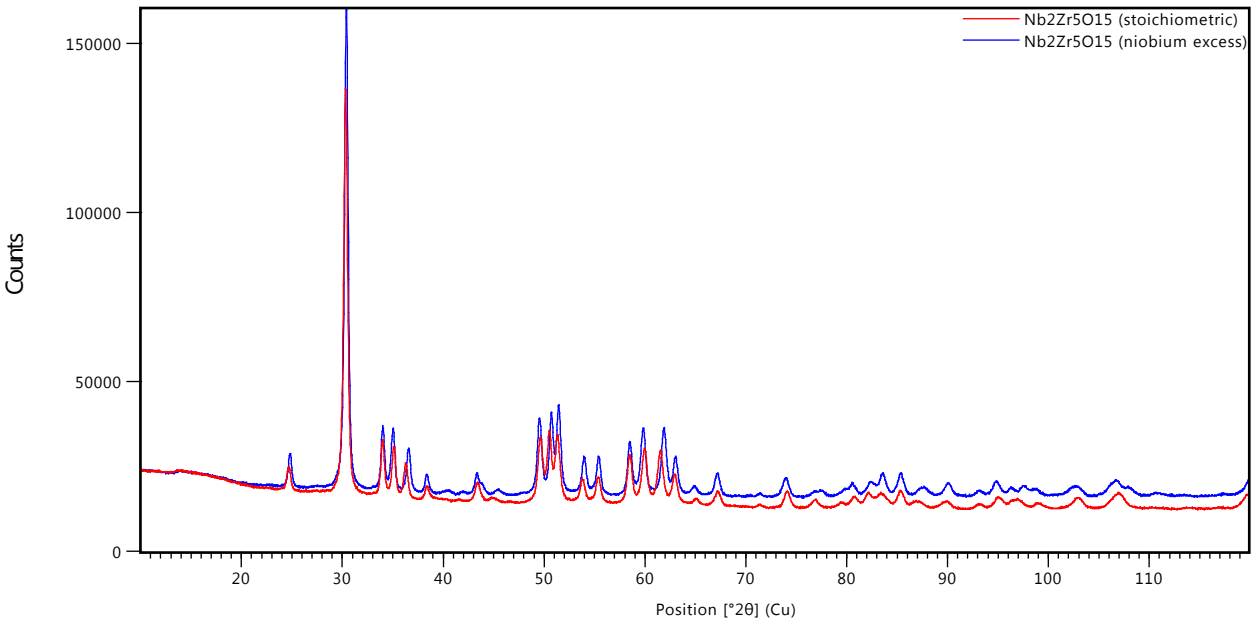

Figure S8. Diffractograms of $Nb_2Zr_5O_{15}$ synthesized with (blue) and without niobium excess (red).

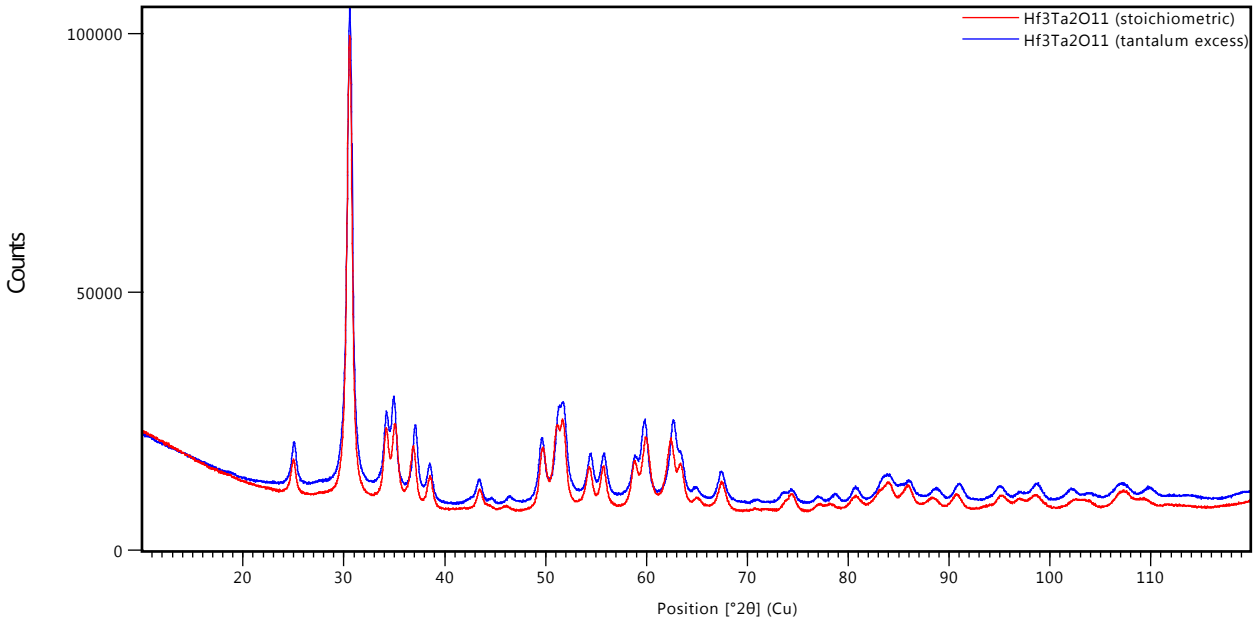

Figure S9. Diffractograms of $Hf_3Ta_2O_{11}$ synthesized with (blue) and without tantalum excess (red).

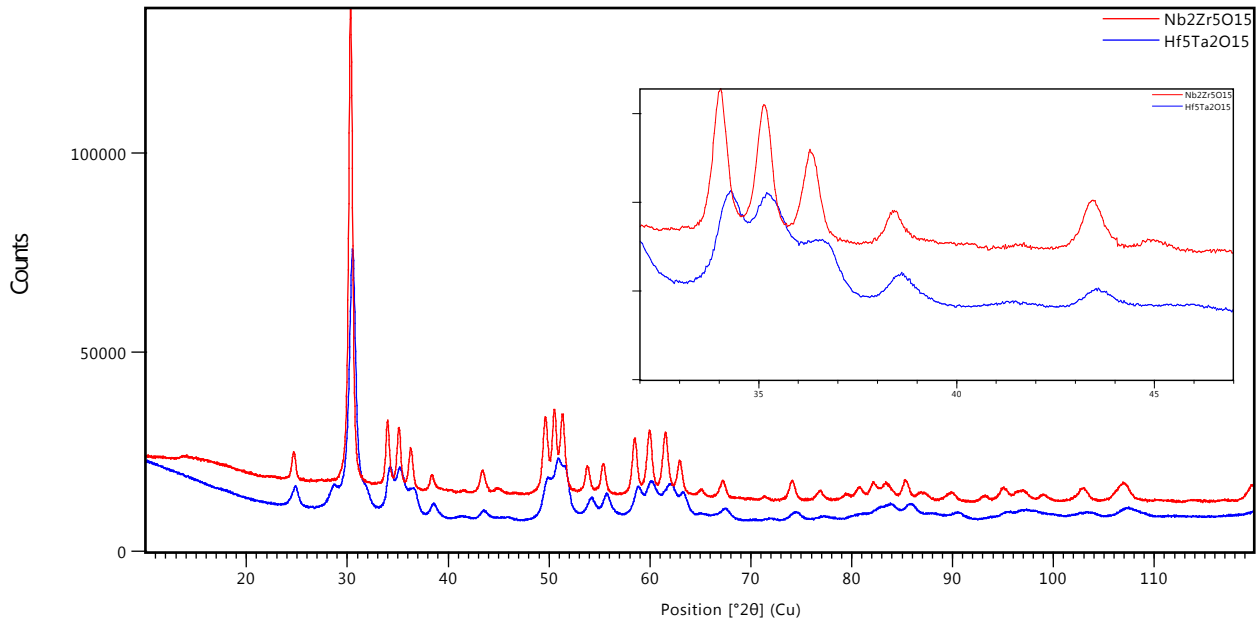

Figure S10. Diffractograms of $Nb_2Zr_5O_{15}$ (red) and tentative $Hf_5Ta_2O_{15}$ (blue) with detail of the range $32° \leq 2\theta \leq 47°$ (inset). Reflections are much broader for the heavier homologue, indicating lower crystallinity and hindering further analysis.

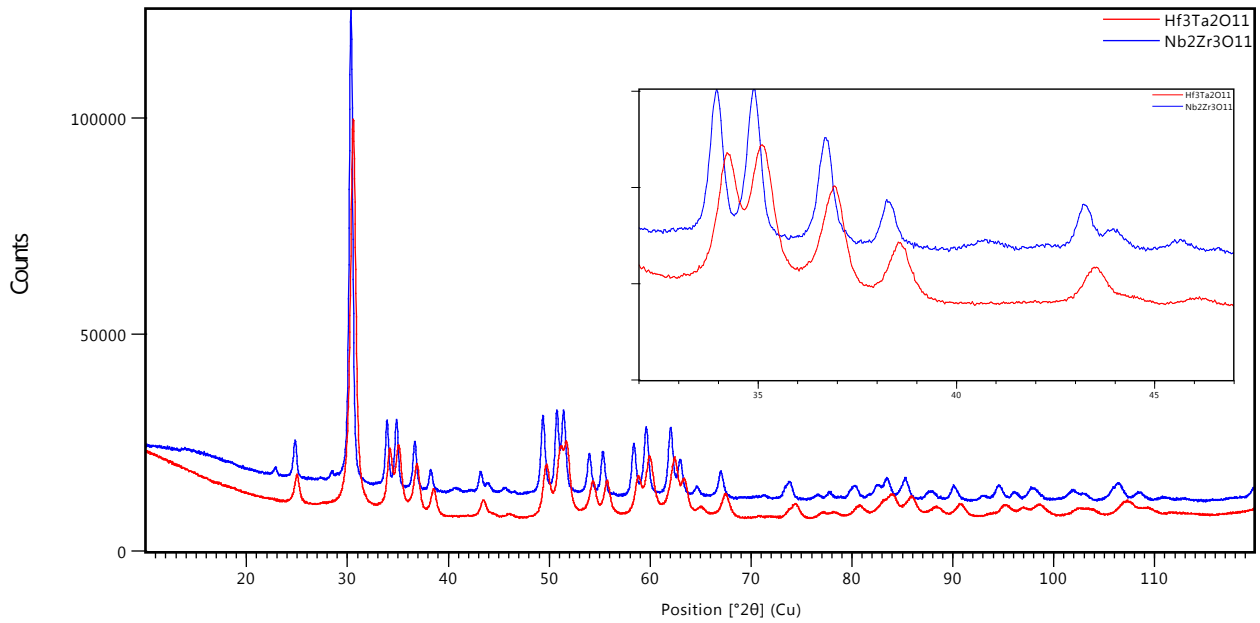

Figure S11. Diffractograms of "$Nb_2Zr_3O_{11}$" (blue) and $Hf_3Ta_2O_{11}$ (red) with detail of the range $32° \leq 2\theta \leq 47°$ (inset). Additional reflections, for which satellites cannot account, appear at *ca.* 22.9 and 28.5°.

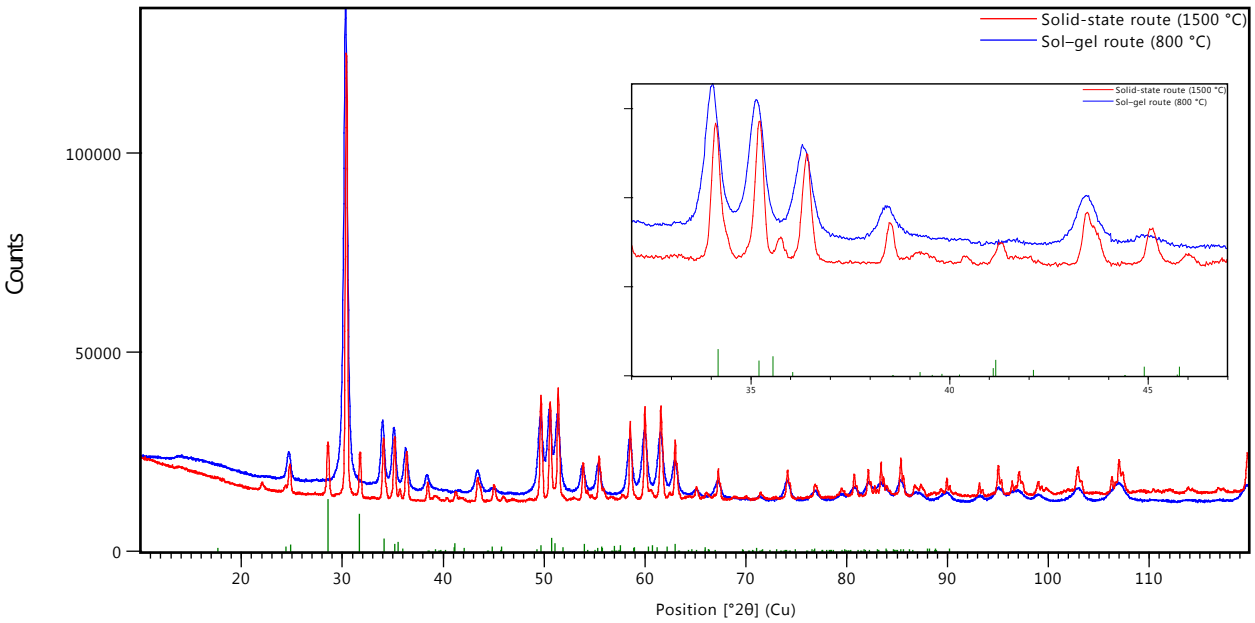

Figure S12. Diffractograms of products of attempted $Nb_2Zr_5O_{15}$ syntheses *via* a solid-state (red) and a sol–gel route (blue) starting from stoichiometric precursor amounts with detail of the range $32° \leq 2\theta \leq 47°$ (inset). In the diffractogram after solid-state synthesis, additional reflections show the presence of baddeleyite-type ZrO_2 (green indicators)[13] and another unknown minor phase (at *ca.* 22.1°).

5 References

[1] M. P. Pechini (Sprague Electric Company), US-A 3330697, **1967**.

[2] M. Hoelzel, A. Senyshyn, O. Dolotko, *J. Large-Scale Res. Facil.* **2015**, *1*, A5.

[3] M. Hoelzel, A. Senyshyn, N. Juenke, H. Boysen, W. Schmahl, H. Fuess, *Nucl. Instrum. Methods Phys. Res., Sect. A* **2012**, *667*, 32–37.

[4] V. Petříček, M. Dušek, L. Palatinus, *Z. Kristallogr. – Cryst. Mater.* **2014**, *229*, 345–352.

[5] L. W. Finger, D. E. Cox, A. P. Jephcoat, *J. Appl. Crystallogr.* **1994**, *27*, 892–900.

[6] A. Leineweber, V. Petříček, *J. Appl. Crystallogr.* **2007**, *40*, 1027–1034.

[7] D. Wiedemann, T. Lüdtke, L. Palatinus, E. Willinger, M. G. Willinger, M. J. Mühlbauer, M. Lerch, *Inorg. Chem.* **2018**, *57*, 14435–14442.

[8] K. Brandenburg, Diamond, Crystal and Molecular Structure Visualization, Crystal Impact – H. Putz & K. Brandenburg GbR, Bonn, Germany, **2018**.

[9] J.-F. Bérar, G. Baldinozzi, *J. Appl. Crystallogr.* **1993**, *26*, 128–129.

[10] a) P. J. Brown, A. G. Fox, E. N. Maslen, M. A. O'Keefe, B. T. M. Willis, in *International Tables for Crystallography, Vol. C* (Ed.: E. Prince), John Wiley & Sons, Hoboken, New Jersey, USA, **2006**, pp. 554–590; b) E. Hovestreydt, *Acta Crystallogr., Sect. A: Found. Crystallogr.* **1983**, *39*, 268–269.

[11] OriginLab, OriginPro, Data Analysis and Graphing Software, OriginLab Corp., Northampton, USA, **2018**.

[12] T. Degen, M. Sadki, E. Bron, U. König, G. Nénert, *Powder Diffraction* **2014**, *29*, S13-S18.

[13] C. J. Howard, E. H. Kisi, R. B. Roberts, R. J. Hill, *J. Am. Ceram. Soc.* **1990**, *73*, 2828–2833.